S-Layer Proteins as Key Components of a Versatile Molecular Construction Kit for Biomedical Nanotechnology

B. Schuster*, D. Pum, M. Sára and U.B. Sleytr

Center for NanoBiotechnology, University of Natural Resources and Applied Life Sciences, 1180 Vienna, Austria

Abstract: Surface (S)-layer proteins and S-layer fusion proteins incorporating functional sequences, self-assemble into monomolecular lattices on solid supports and on various lipid structures. Based on these S-layer proteins, supramolecular assemblies can be constructed which are envisaged for label-free detection systems, as affinity matrix, as anti-allergic immuno-therapeutics, as membrane protein-based screening devices, and as drug targeting and delivery systems.

Keywords: Crystalline surface layer proteins, artificial virus, biomimetics, bottom-up strategy, S-layer fusion protein, microspheres-based detoxification system, nanobiotechnology.

1. INTRODUCTION

The cross fertilization of biology, molecular biology, organic chemistry, material sciences, and physics has opened up significant opportunities for innovation in previously unrelated fields. In this context, self-assembly is a new and rapidly growing scientific and engineering discipline that crosses the boundaries of numerous existing fields. Self-assembly can be defined as a "bottom-up" process by which individual molecules (ranging in size up to large polymers) become spontaneously organized into supramolecular structures. This alternative to "top-down" processing steps can lead to both, new materials and structures that are not obtained by conventional techniques, and to the ultimate miniaturization of functional units.

One of the great challenges for nano(bio)technology is the creation of supramolecular materials in which the constituent units are highly regular molecular nanostructures. Thus, learning how to create complex and large supra-molecular structures and the elucidation of rules mediating their organization into functional materials will offer a broad spectrum of new technologies.

It is now well-recognized that crystalline bacterial cell surface layers (S-layers) composed of identical proteinaceous subunits represent unique patterning elements and scaffolding structures for nanobiotechnological applications. The possibility for incorporating single or multifunctional domains to S-layer proteins by genetic engineering has led to ultimate control and precision in the spatial distribution and orientation of molecules and functional domains as required for life- and non-life science applications. Most relevant, S-layers represent the base for very versatile self-assembly systems involving all major species of biological molecules such as proteins, lipids, glycans, nucleic acids, and combination of that.

*Address correspondence to this author at the Center for Nano-Biotechnology, University of Natural Resources and Applied Life Sciences Vienna, Gregor-Mendel-Strasse 33, 1180 Vienna, Austria; Tel: ++43-1-47654-2200; Fax: ++43-1-4789112; E-mail: bernhard.schuster@boku.ac.at

2. GENERAL ASPECTS OF S-LAYER PROTEINS

Crystalline bacterial cell surface layers, referred to as S-layers [1-3] have now been identified in hundreds of different species of bacteria and represent an almost universal feature of archaea (Fig. **1**) [for reviews see 2, 4-10]. Since S-layers are composed of a single protein or glycoprotein species endowed with the ability to assemble into a monomolecular lattice during all stages of cell growth and cell division, they can be considered as the simplest type of biological membranes developed in the course of evolution [for review see 11].

S-layers can be associated with quite different supporting supramolecular structures. In most archaea, S-layers represent the only wall component and can be so closely associated with the plasma membrane that a hydrophobic domain of the constituent subunits is actually integrated into the lipid layer [6, 8, 12]. In most Gram-positive bacteria the S-layer is attached to a rigid wall matrix involving lectin binding between a glycan (referred to as secondary cell wall polymer, SCWP) covalently-attached to the peptidoglycan meshwork [13]. In Gram-negative bacterial cell envelopes S-layers are linked to the lipopolysaccharide component of the outer membrane. In most prokaryotic organisms S-layers have to be considered as non-conservative structures with the potential to fulfil a broad spectrum of functions [3, 4, 9]. Considering that S-layer carrying organisms are ubiquitous in the biosphere and even dwell under the most extreme environmental conditions, the supramolecular concept of a dynamic closed crystalline surface layer could have the potential to fulfil a broad spectrum of functions. Because S-layer lattices possess pores identical in size and morphology in the 2 to 8 nm range, they work as precise molecular sieves providing sharp cut off levels for the bacterial cell [14]. As isoporous ultrafiltration membrane they can apparently provide the microorganisms with a selection advantage by functioning as protective coats, molecule and ion traps, and as a structure involved in cell adhesion, surface recognition or antifouling [5, 11, 12, 15]. In those archaea which possess S-layers as exclusive envelope component outside the cytoplasmic membrane, the crystalline array acts as a frame

1389-5575/06 $50.00+.00

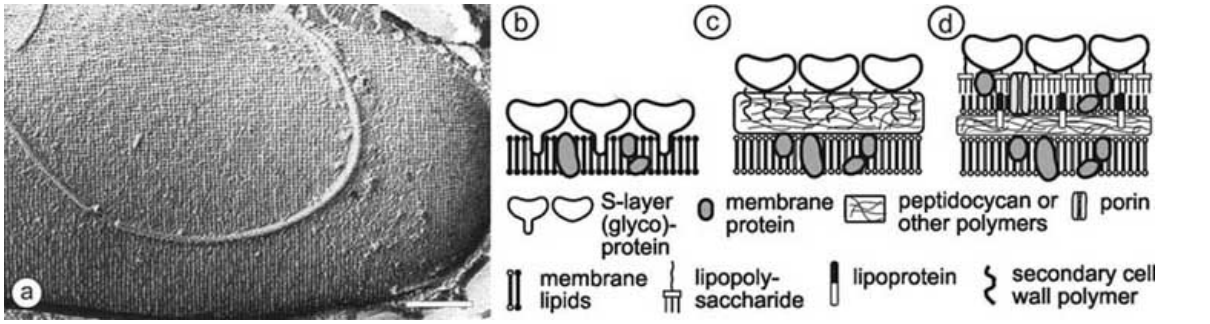

Fig. (1). In (a), freeze-etching preparation of a whole cell of *Bacillus sphaericus* with a square S-layer lattice is shown. Bar corresponds to 200 nm. Schematic illustration of the supramolecular architecture of the three major classes of prokaryotic cell envelopes containing crystalline bacterial cell surface layers (S-layers). (b) Cell envelope structure of gram-negative archaea with S-layers as the only component external to the cytoplasmic membrane. (c) Cell envelope as observed in gram-positive archaea and bacteria. In bacteria the rigid wall component is primarily composed of peptidoglycan. In archaea other wall polymers (e.g. pseudomurein) are found. (d) Cell envelope profile of gram-negative bacteria composed of a thin peptidoglycan layer and an outer membrane. If present, the S-layer is closely associated with the lipopolysaccharide of the outer membrane. Modified after Ref. [5], Copyright (1999) with permission from Wiley-VCH.

work that determines and maintains the cell shape and stabilizes the cytoplasmic membrane [16, 17].

From a general point of view S-layers as the most abundant of bacterial cellular proteins are important model systems for studying the structure, synthesis, assembly, and function of these proteinaceous components. The investigation of the general principles of S-layers also have revealed considerable application potential in biotechnology, biomimetics, and nano(bio)technology [11, 15, 18-21].

2.1. Structural Analysis of S-Layer Lattices

High resolution transmission electron microscopy (TEM) and scanning force microscopy (SFM) are commonly used to characterize S-layer protein lattices. In particular, in TEM the appropriate preparation method is most important for investigating the ultrastructure of S-layer protein lattices at molecular resolution (Fig. **1**). Freeze-etching and freeze-drying in combination with heavy metal shadowing are the most straight forward approaches for obtaining information about the lattice type and surface structure of S-layers on bacterial cells and S-layer cell wall fragments [1, 22]. These studies revealed that many S-layers show a smooth outer and a more corrugated inner face [23, 24]. This difference is of particular importance when the orientation (sidedness due to attachment of the S-layer subunits *via* the inner or outer surface) of S-layers on artificial substrates has to be determined. Nevertheless, TEM of frozen hydrated specimens [23-25] yields the highest resolution among all microscopical techniques. In plane, a resolution of 0.35 nm and in the third dimension 0.7 nm is attainable. In three-dimensional TEM, tilt series of the specimen is recorded under low electron dose conditions (usually not more than 1 to 2 electrons per $Å^2$). Although quantum noise governs image formation, such low electron doses are mandatory in order to maintain the three-dimensional structure of the proteins [25]. Image processing methods are used to enhance the signal-to-noise ratio in low dose micrographs.

Negative staining is an easy preparation technique in TEM. Particularly in combination with two and three dimensional image reconstruction techniques, it allows high resolution studies of the ultrastructure of S-layer lattices [23-25].

Contrary to the electron microscopical preparation techniques, scanning force microscopy allows to investigate S-layer monolayers in their native environment [26-28]. Contact mode microscopy in liquid is most frequently used to investigate S-layer protein monolayers at sub-nanometer resolution. S-layer proteins are highly susceptible towards the applied tip loading forces which shall not exceed 0.5 to 1 nN. Ionic content and strength of the buffer solution in the liquid cell has to be carefully adjusted in order to minimize electrostatic interactions between tip and sample. Silicon wafers and mica are the most commonly used substrates for scanning force microscopical investigations since these provide hard and very flat surfaces. In particular, silicon surfaces are most relevant for nanobiotechnological applications. S-layer proteins recrystallize into large scale monomolecular protein lattices on silicon, whereas S-layer fragments or self-assembly products are preferably deposited on mica. If S-layer proteins are recrystallized on flat solid supports such as silicon wafers, lattice formation can be followed in real time [26]. It could be demonstrated that crystal growth starts at several distant nucleation points and proceeds in-plane until a closed layer of crystalline domains is formed [26]. The scanning force microscope has been also used as a nano-tool for inducing conformational changes in S-layer proteins [29, 30]. Furthermore, the capability of scanning force microscopy to resolve molecular details on biological samples together with its force detection sensitivity has led to the development of the so-called "topography and recognition mode", a method suitable for visualizing the chemical composition of a sample while mapping its topography [31]. It is anticipated that the simultaneous investigation of both, topography and recognition, will allow to elucidate the structure-function relationship of a broad spectrum of biological samples in an unsurpassed way.

2.2. Self-assembly Properties of S-Layer Proteins

While many archaeal S-layer proteins are covalently anchored, those of bacteria are non- covalently linked to each other and to the supporting cell wall component. Thus, a complete solubilization of S-layers into their constituent subunits and release from the bacterial cell envelope can be

achieved by treatment with high concentrations of hydrogen-bond breaking agents (e. g. urea, guanidinium hydrochloride), by dramatic changes in the pH-value or in the salt concentration. Upon removal of the disrupting agent, e. g. by dialysis, S-layer proteins self-assemble into two dimensional arrays [for review see ref. 32]. Such self-assembly products may have the form of flat sheets or open-ended cylinders. Depending on the particular S-layer protein species used and on the environmental conditions, monolayers or double layers are formed.

Contrary to the reassembly in solution, prior to recrystallization on artificial supports, S-layer proteins must be kept in a water soluble state. This can either be achieved in the absence of bivalent cations [33] or by maintaining a sub-critical protein concentration for self-assembly [34]. In addition, in the presence of S-layer-specific SCWPs, the reassembly in suspension is inhibited, whereas the recrystallization of soluble S-layer proteins on artificial supports is promoted [13, 34, 35]. The formation of coherent crystalline arrays strongly depends on the S-layer protein species, the environmental conditions of the bulk phase (e. g. temperature, pH-value, ion composition and ionic strength) and, in particular, on the surface properties of the substrate. For example, the S-layer protein SbpA of *Bacillus sphaericus* CCM2177 forms double layers with perfect long range order (up to several micrometers in diameter) on hydrophilic silicon but monolayers consisting of 200 to 500 nm sized patches on hydrophobic silicon.

In accordance with S-layer proteins recrystallized on solid substrates, the orientation of the protein arrays (sidedness due to the attachment *via* the inner or outer surface of the S-layer subunits) at liquid interfaces and at lipid films is determined by the anisotropy in the physicochemical surface properties of the protein lattice [for review see ref. 36]. For example, the S-layer protein SbsB of *Geobacillus stearothermophilus* pv72/p2 reassembles with its more hydrophobic outer face at the air-water interfaces while at lipid films with zwitterionic head groups the S-layer lattice is attached with its inner face [37]. The unambiguous determination of the orientation of the S-layer is possible since it shows oblique lattice symmetry with a characteristic handedness of the proteins. In addition to the formation of flat S-layer lattices it has also been demonstrated that S-layer proteins are able to cover liposomes and nanocapsules completely [38-49]. The S-layer shows facets and numerous lattice faults in order to follow the curvature of the spheres. According to the observations with planar lipid films, the charge of the lipid head groups and the polyelectrolyte determines the orientation of the S-layer protein against the liposome and the nanocapsule, respectively [41, 42].

2.3. Chemical Properties and Molecular Biology of S-layer Proteins

Chemical analyses and genetic studies revealed that the S-layer lattices are composed of a single homogeneous protein or glycoprotein species with a molecular mass ranging from 40 to 200 kDa [5, 9, 11, 43]. Most S-layer proteins are weakly acidic with isoelectric points in the range of 4 to 6 [9]. In general, S-layer proteins consist of a large portion of hydrophobic amino acids (40 - 60 mol %), about 25 mol % are charged amino acids, and S-layer proteins possess little or no sulfur-containing amino acids. Secondary structure predictions of S-layer proteins indicate that about 40 % occur as β-sheets and approximately 20 % of the amino acids are organized as α-helices. Most α-helical segments are arranged in the N-terminal part. Aperiodic foldings and β-turn content may vary between 5 % and 45 %.

In order to elucidate the structure-function relationship of distinct segments of S-layer proteins, N- and / or C-terminally truncated forms were produced and their self-assembly and recrystallization properties investigated [44-46]. Another approach was seen in performing a cysteine scanning mutagenesis and screening the accessibility of the single introduced cysteine residue in the soluble, self-assembled and recrystallized S-layer proteins [34]. This study elucidated which amino acid positions in the primary sequence are located on the outer or inner S-layer surface of the subunits, inside the pores, or at the subunit to subunit interface.

The fact that no structural model at atomic resolution of an S-layer protein is available until now, may be explained by the molecular mass of the subunits being too large for nuclear magnetic resonance analysis, as well as by the intrinsic property of S-layer proteins to self-assemble into two dimensional lattices, thereby hindering the formation of isotropic three dimensional crystals as required for X-ray crystallography. In addition, the low solubility of S-layer proteins is a general hindrance for both methods.

In the case of the S-layer protein SbsC of *G. stearothermophilus* ATCC 12980, water soluble N- or C-terminally truncated forms were used for first three dimensional crystallization studies. Crystals of the C-terminally truncated $rSbsC_{31-844}$ diffracted to a resolution of 3 Å using synchrotron radiation [47]. Native and heavy atom derivative data confirmed the results that the N-terminal region is mainly organized as α-helices, whereas the middle and C-terminal part of SbsC consist of loops and ß-sheets [47].

The N-terminal region was found to be responsible for anchoring the S-layer subunits to the underlying rigid cell envelope layer by binding to the SCWP. The polymer chains are covalently linked to the peptidoglycan backbone which occurs most probably *via* phosphodiester bonds [48]. Basically, two types of binding mechanisms between the N-terminal part of S-layer proteins and SCWPs have been described [49]. The first one, which involves so-called S-layer-homologous (SLH) domains and pyruvylated SCWPs [33, 40, 44, 50, 51] has been found to be widespread among prokaryotes and is considered as having been conserved in the course of evolution [51]. The second type of binding mechanism has been described for *G. stearothermophilus* PV72/p6 and ATCC 12980 [9, 52, 53], a temperature-derived strain variant from the latter [54], and *G. stearothermophilus* NRS 2004/3a [55]. This binding mechanism involves an SCWP that consists of N-acetyl glucosamine, glucose and 2,3-dideoxy-diacetamido-D-mannosamine uronic acid in the molar ratio of 1:1:2 (see compound (**1**) in Fig. **2**) [55, 56] and a highly conserved N-terminal region which does not possess an SLH-domain [52-55]. Concerning the first binding mechanism, the construction of knock-out mutants

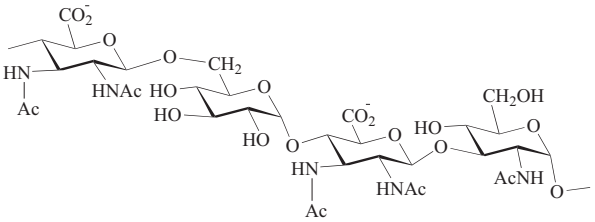

[-4)-β-DMan*p*A2,3(NAc)$_2$-(1-6)-α-D-Glc*p*-(1-4)-β-D-Man*p*A2,3(NAc)$_2$-(1-3)-α-DGlc*p*NAc-(1-] (**1**)

Fig. (2). Chemical structure of the repeating unit of the secondary cell wall polymer of *G. stearothermophilus* NRS 2004/3a (**1**).

in *Bacillus anthracis* and *Thermus thermophilus* in which the gene encoding a putative pyruvyl transferase was deleted demonstrated that the addition of pyruvic acid residues to the peptidoglycan-associated cell wall polymer was a necessary modification to bind SLH-domain containing proteins [50, 51].

3. A MOLECULAR CONSTRUCTION KIT BASED ON S-LAYER PROTEINS

The biomimetic approach learning from nature how to create supramolecular, layered structures by a bottom-up process is one of the most challenging scientific tasks in nanobiotechnology. Advantage can be taken of the self-assembling nature of S-layer (fusion) proteins, SCWPs and natural and/or artificial lipids and their properties in the compartmentalization of components in nanoscale regions, production of self-assembling biomaterials, construction of drug-targeting and delivery systems, and development of smart biosensors [18, 19, 57-59].

3.1. S-Layer Fusion Proteins and their Application Potentials

So far, the chimaeric genes encoding several S-layer fusion proteins have been heterologously expressed in *Escherichia coli*. S-layer fusion proteins were based on the S-layer proteins SbsB, SbsC, and SbpA (Table **1**). SbsB forms an oblique S-layer lattice with p1 symmetry and lattice parameters of a = 10.4 nm, b = 7.9 nm and a base angle of γ = 81°, whereas SbpA assembles into a square lattice with a lattice constant of 13.1 nm.

For generating a universal affinity matrix for binding any kind of biotinylated molecule, S-layer-streptavidin fusion proteins were constructed [60, 61]. Minimum-sized core streptavidin (118 amino acids) was either fused to N- or C-terminal positions of SbsB or to the C-terminal end of rSbpA$_{31\text{-}1068}$ [45, 61].

The genes encoding the fusion proteins and core streptavidin were expressed independently in *E. coli* and isolated from the host cells. To obtain functional hetero-tetramers (HTs), a refolding procedure was developed by subjecting a mixture of fusion protein with excess core streptavidin to denaturing and renaturing conditions and isolating functional HTs by size exclusion and affinity chromatography. HTs comprising the N-terminal rSbsB-streptavidin formed self-assembly products in suspension and recrystallized on liposomes and silicon wafers [61], whereas HTs based on the C-terminal rSbpA$_{31\text{-}1068}$-streptavidin fusion protein showed dirigible self-assembly formation, as lattice formation of SbpA is strongly dependent on the presence of calcium ions. HTs based on the rSbpA$_{31\text{-}1068}$-streptavidin fusion protein recrystallized on gold surfaces that were optionally pre-coated with SCWP [60]. Analysis of negatively-stained preparations of self-assembly products formed by HTs revealed that neither the oblique S-layer

Table 1. Summary of Various S-Layer Fusion Proteins (Selected from Various Constructs)

S-layer fusion protein	Length of functionality	Functionality	Reference
rSbsB / core streptavidin rSbpA$_{31\text{-}1068}$ / core streptavidin	118 aa	biotin binding	[45, 60, 61]
rSbsC$_{31\text{-}920}$ / Bet v1 rSbpA$_{31\text{-}1068}$ / Bet v1	116 aa	major birch pollen allergen	[45, 66]
rSbpA / Strep-tag I rSbpA$_{31\text{-}1068}$ / Strep-tag I	9 aa	affinity tag for streptavidin	[45]
rSbpA$_{31\text{-}1068}$ / ZZ	116 aa	IgG-binding domain	[64]
rSbpA$_{31\text{-}1068}$ / GFP	238 aa	green fluorescent protein	[68]
rSbpA$_{31\text{-}1068}$ / cAb	117 aa	heavy chain camel antibody	[62, 63]

Mature proteins: *Bacillus sphaericus* CCM2177 variant A (SbpA): 1238 amino acids (aa); *Geobacillus stearothermophilus* pv72/p2 (SbsB): 889 aa; *Bacillus stearothermophilus* ATCC 12980 (SbsC): 1099 aa.

lattice of SbsB, nor the square lattice of SbpA had changed due to the presence of the fusion partner. Digital image reconstructions of self-assembly products of HTs comprising the N-terminal rSbsB-streptavidin fusion protein showed an additional protein mass on the N-terminal SLH-domain which resulted from the fused streptavidin moiety [61]. As a first application approach, monolayers of HTs based on $rSbpA_{31-1068}$ were recrystallized on plain gold chips and on those pre-coated with thiolated SbpA-specific SCWP, and the obtained affinity matrix was used to perform hybridization experiments. In a first step, biotinylated oligonucleotides (30-mers) were bound to the streptavidin moiety of the HTs, and complementary oligonucleotides were hybridized carrying no or one mismatch [60]. Evaluation of the hybridization experiments was performed by applying surface-plasmon-field-enhanced fluorescence spectroscopy which combines the advantages of the high optical field intensities of surface plasmon waves with the sensitive detection of fluorescence light emission. For hybridization experiments on monolayers generated by recrystallization of HTs on gold chips pre-coated with thiolated SCWP, fluorescently labelled oligonucleotides carrying one mismatch were used. The fluorescence intensity increased linearly at the beginning of the hybridization reaction, so that the linear slope of the increase in the fluorescence intensity plotted versus the concentration of the hybridizing oligonucleotides led to a linear correlation [60]. In a different set of hybridization experiments which were performed on monolayers generated by direct recrystallization of HTs on plain gold chips, the concentration of oligonucleotides carrying one mismatch was step-wise increased. The Langmuir isotherm which indicated that oligonucleotides in solution were in equilibrium with those bound to the monolayer carrying the biotinylated oligonucleotides could be established from the obtained fluorescence intensities [60]. The detection limit was found to be 1.57 pM on monolayers generated by recrystallization of HTs on gold chips pre-coated with thiolated SCWP, whereas on plain gold chips, the detection limit was determined to be at least 8.2 pM. To conclude, the hybridization experiments indicated that a functional sensor surface could be generated by recrystallization of HTs on gold chips, which could find numerous applications in (nano)biotechnology.

An S-layer fusion protein comprising the C-terminally truncated form $rSbpA_{31-1068}$ and the variable region of a heavy chain camel antibody directed against lysozyme was constructed. The Camelidae is the only taxonomic family known to possess functional heavy chain antibodies lacking light chains and the first constant region. These unique antibody isotypes interact with the antigen by virtue of a single variable domain, termed VHH. A single VHH domain has a molecular mass of only 15,000 and is the smallest known complete antigen binding fragment from a functional immunoglobulin. As proof-of-principle was provided with a fusion protein comprising a VHH directed against lysozyme [62], an S-layer fusion protein incorporating the sequence of a variable domain of a heavy chain camel antibody (cAb-PSA-N7) directed against the prostate-specific antigen (PSA) was constructed [63]. PSA is a useful marker to screen potential prostate cancer patients. The current diagnostic test systems determine the concentration of total PSA with monoclonal antibodies that recognize free, as well as PSA complexed with alpha-1-anti-chymotrypsin. For application in a PSA biosensor, VHHs recognizing free and complexed PSA are desired. Moreover, kinetic requirements in the biosensor impose a high probe density that can probably only be obtained with single domain VHHs.

To generate a PSA-specific sensing layer for SPR measurements, the S-layer fusion protein $rSbpA_{31-1068}$/cAb-PSA-N7 was recrystallized on gold chips pre-coated with thiolated SCWP. The formation of the monomolecular protein lattice was confirmed by scanning force microscopy, as well as by the level of the measured SPR signal. As derived from response levels measured for binding of PSA to a monolayer consisting of $rSbpA_{31-1068}$ /cAb-PSA-N7, the molar ratio between bound PSA and the S-layer fusion protein was 0.78, which means that at least three PSA molecules were bound per morphological unit of the square S-layer lattice with an area of ~ 170 nm^2. To summarize, by using SbpA-specific SCWP as biomimetic linker to gold chips, a sensing layer for SPR could be generated by recrystallization of this S-layer fusion protein. Due to the crystalline structure of the S-layer lattice, the fused ligands showed a well defined distance in the protein lattice, and according to the selected fusion site in the S-layer protein, they were located on the outermost surface, which should reduce diffusion limited reactions. A further advantage can be seen in the constant and low distance of the ligands from the optically active gold layer, which is exclusively determined by the thickness of the S-layer and lies in the range of only 10 to 15 nm. Thus, S-layer fusion proteins incorporating camel antibody sequences can be considered as key element for the development of label free detection systems such as SPR, surface acoustic wave, or quartz crystal microbalance, in which the binding event can be measured directly by the mass increase without the need of any labelled molecule.

The sequence encoding $rSbpA_{31-1068}$ was also used as base form for the construction of an IgG-binding fusion protein [64]. As fusion partner, the sequence encoding the Z-domain, a synthetic analogue of the IgG-binding domain of Protein A from *Staphylococcus aureus*, was used. To generate the S-layer fusion protein, the 5′-end of the sequence encoding two copies of the Z-domain was fused *via* a short linker to the gene encoding $rSbpA_{31-1068}$. After heterologous expression in *E. coli*, the S-layer fusion protein was isolated from the host cells, purified by size exclusion chromatography under denaturing conditions, dialysed and recrystallized on gold chips which were pre-coated with thiolated SbpA-specific SCWP. As shown by scanning force microscopy, a monomolecular protein lattice with square symmetry was formed. Native monolayers or monolayers cross-linked with the bifunctional imidoester dimethylpimelimidate (DMP, compound (**2**)) (Fig. **3**) were finally exploited for binding of human IgG. The amount that could be bound by the native monolayer was 2.9 x 10^{-5} nM or 4.35 ng IgG / mm^2, whereas in the case of the DMP-cross-linked monolayer (Fig. **3**) 2.8 x 10^{-5} nM or 4.20 ng IgG / mm^2 could attach. These values corresponded to 65 and 67 % of the theoretical saturation capacity of a planar surface for IgG (6.5 ng / mm^2) with the Fab regions occurring in the

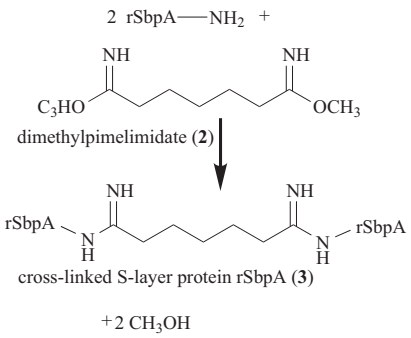

Fig. (3). Cross-linking of the recombinant S-layer protein rSbpA with the homobifunctional imidoester dimethylpimelimidate (DMP; compound (**2**)). The spacer arm length of DMP is 0.92 nm.

condensed state. As derived from these binding capacities, on average 2.7 and 2.6 IgG molecules were bound per morphological unit of the square S-layer lattice consisting of four identical subunits of the S-layer fusion protein. For preparing biocompatible microparticles for the microspheres-based detoxification system (MDS) [65] to remove auto-antibodies from patients´ sera suffering from auto-immune disease, the S-layer fusion protein was recrystallized on SCWP-coated, 3 µm large cellulose-based microbeads (Fig. **4**). The MDS is an alternative approach to conventional immunoadsorption systems, in which the plasma does not perfuse on an adsorption column, but is recirculated into a filtrate compartment of a membrane module. The addition of microbeads to the plasma circuit would allow the rapid removal of the pathogenic substrates. In the case of microbeads that were covered with a native monolayer, the binding capacity was 1,065 µg human IgG / mg S-layer fusion protein. For DMP-treated microbeads, a binding capacity of 870 µg IgG / mg S-layer fusion protein was determined. These values corresponded to 78 or 65 % of the theoretical saturation capacity of a planar surface for IgG having the Fab regions in the condensed state. Bound IgG could be eluted with glycine-HCl buffer at a pH value of 2.2 and the microbeads were used for further IgG-binding experiments [64].

The major birch pollen allergen Bet v1 shares IgE epitopes with all tree pollen allergens from closely related species (e. g. alder hazel, hornbeam, beech). Because of high sequence identities among these allergens and well studied cross-reactions with B-cell epitopes, Bet v1 represents a model allergen. The gene encoding the chimaeric S-layer proteins rSbsC$_{31\text{-}920}$/Bet v1 [64] and rSbpA$_{31\text{-}1068}$/Bet v1 [45] carrying Bet v1 at the C-terminal end were cloned and expressed in *E. coli*. In a recent study, the applicability of rSbsC$_{31\text{-}920}$/Bet v1 as a novel approach to design vaccines with reduced allergenicity in combination with strong immune-modulating capacity for immunotherapy of type I allergy could be demonstrated [67]. This fusion protein exhibited all relevant Bet v1-specific B and T cell epitopes, but was significant less efficient in releasing histamine than free Bet v1. In cells of birch pollen-allergic individuals, the fusion protein was capable of modulating the allergen-specific Th2-dominated response into a more balanced Th1/Th0-like phenotype accompanied by enhanced production of IFN-γ and IL-10. To conclude, rSbsC$_{31\text{-}920}$/Bet v1 could find application as carrier/adjuvants to design vaccines for specific immunotherapy of type 1 allergy with improved efficacy and safety [67].

The nucleotide sequence encoding enhanced green fluorescent protein (EGFP), a red-shifted green fluorescent protein (GFP)-derivative possessing a 30 times brighter fluorescence intensity at 488 nm than wild-type GFP was fused to the 3´end of the sequence encoding the C-terminally truncated form rSbpA$_{31\text{-}1068}$ [68]. The chimaeric gene encoding rSbpA$_{31\text{-}1068}$/EGFP was expressed in *E. coli*, whereby expression at 28°C instead of 37°C resulted in clearly increased fluorescence intensity, indicating that the folding process of the EGFP moiety was temperature sensitive. Comparison of excitation and emission spectra of rEGFP and rSbpA$_{31\text{-}1068}$/EGFP indicated identical maxima at 488 and 507 nm, respectively. Furthermore, this fusion protein was used for recrystallization on silicon wafers covered with polyelectrolytes, as well as for coating of hollow polyelectrolyte capsules. Fluorescence spectroscopy confirmed that the adsorption of rSbpA$_{31\text{-}1068}$/EGFP on hollow capsules did not shift the fluorescence emission of the chromophore [41]. Finally, the recrystallization of this

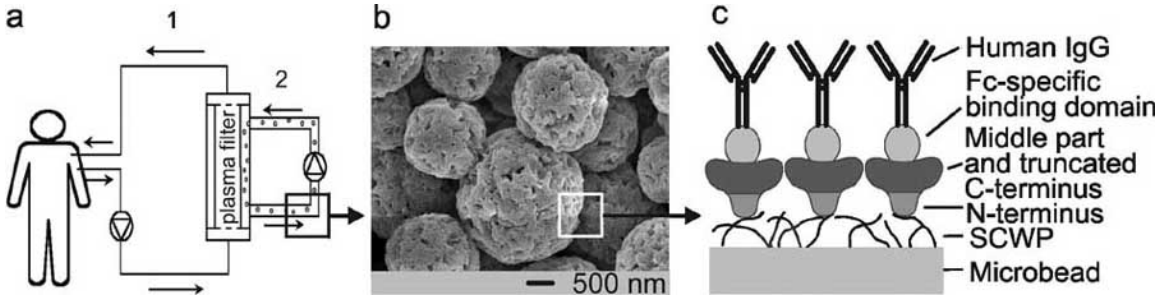

Fig. (4). (a) Schematic drawing of the MDS, showing the primary circuit (labelled 1) containing the whole blood of the patient. The blood cells are rejected by the plasma filter. In the second circuit (labelled 2), the plasma re-circulates together with the S-layer fusion protein-coated microbeads, on which IgG is bound. After passing the plasma filter again, the purified plasma is combined with blood cells, and the whole blood is re-infused into the patient. (b) Scanning electron micrograph of the cellulose-based microbeads used for recrystallization of rSbpA$_{31\text{-}1068}$/ZZ. (c) Schematic drawing showing the oriented recrystallization of the S-layer fusion protein rSbpA$_{31\text{-}1068}$/ZZ on microbeads pre-coated with SCWP and binding of IgG to the ZZ-domains. Reprinted with permission from Ref. [64], Copyright (2004) ASM.

fusion protein on liposomes and their application is described in the following section.

3.2. S-Layer Fusion Proteins on Liposomes as Model for Target Systems

Biomolecular self-assembly can be used as powerful tool for nanoscale engineering. One well known example is the formation of liposomes, which are still very promising supramolecular structures for the application in nanobiotechnology and nanobiomedicine.

Liposomes are colloidal, vesicular structures based on (phospho)lipid bilayers or on tetraetherlipid monolayers [69] and they are widely used as delivery systems for enhancing the efficiency of various biologically active molecules and for the transport of therapeutic agents to the site of disease *in vivo* [70, 71]. Liposomes can encapsulate water soluble agents in their aqueous compartment and lipid soluble substances within the lipid bilayer itself [72]. These agents include small molecular drugs used in cancer chemotherapy and genetic drugs as plasmids encoding therapeutic genes [73]. Generally, liposomes release their contents by interaction with target cells, either by adsorption, endocytosis, lipid exchange or fusion [71, 74].

In previous studies, wild-type SbsB has been recrystallized on positively charged liposomes composed of dipalmitoylphosphatidylcholine, cholesterol and hexadecylamine [38-40, 75]. Such S-layer-coated liposomes (S-liposomes) with a diameter of 50–200 nm represent simple model systems resembling the architecture of artificial virus envelopes (Fig. **5**). For that reason, S-liposomes could reveal a broad application potential, particularly as drug delivery systems or in gene therapy [5].

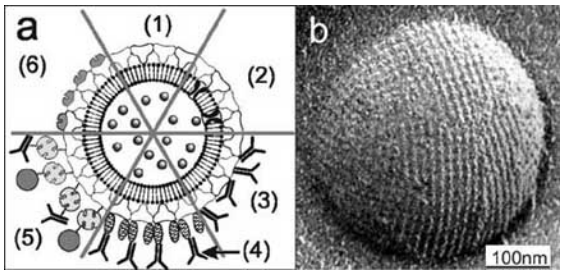

Fig. (5). (a) Schematic drawing of (1) an S-liposome with entrapped functional molecules and (2) functionalized by reconstituted integral proteins. S-liposomes can be used as immobilization matrix for functional molecules (e.g. IgG) either by direct binding (3), by immobilization via the Fc-specific ligand protein A (4), or biotinylated ligands can be bound to the S-liposome via the biotin–streptavidin system (5). (6) Alternatively, liposomes can be coated with genetically modified S layer proteins incorporating functional domains. (b) Electron micrograph of a freeze-etched preparation of an S-liposome. Bar: 100 nm. Reprinted with permission from Ref. [15], Copyright (2002) Wiley-VCH.

S-liposomes possess significantly enhanced stability towards thermal and mechanical stress factors [39]. For generating targeted S-liposomes, the S-layer lattice on liposomes was cross-linked with bis(sulfosuccinimidyl) suberate (BS_3; compound (**4**)) (Fig. **6**), biotinylated and exploited for covalent binding of functional macromolecules, like biotinylated antibodies *via* the streptavidin – biotin bridge [40]. These immuno-S-liposomes comprise several components with specific functions: the liposome as drug carrier, the antibody as homing device, the S-layer lattice as stabilizing structure for the liposome, as anchoring layer for the antibodies, and most probably as stealth coat for prolonged blood circulation times (Fig. **5**).

To avoid chemical modification reactions and to prevent diffusion of potentially toxic agents through the lipid bilayer into the interior of the vesicles, S-layer fusion proteins incorporating the sequence of core–streptavidin have been constructed. Functional streptavidin HTs were prepared as three of the four binding pockets remained accessible for binding biotinylated molecules [61]. After recrystallization of this streptavidin fusion protein on positively charged liposomes, the protein lattice was further functionalized by binding biotinylated peroxidase or biotinylated ferritin [61]. Binding of biotinylated ligands to S-liposomes can be exploited for enabling receptor-mediated uptake into human cells. A further promising application potential can be seen in the development of drug targeting and delivery systems based on lipid-plasmid complexes coated with functional HTs for transfection of human cells.

Another interesting approach can be seen in the generation of a functional chimaeric $rSbpA_{31\text{-}1068}$/EGFP fusion protein to follow the uptake of S-liposomes into mammalian cells [68]. Liposomes coated with a monolayer of $rSbpA_{31\text{-}1068}$/EGFP were incubated with HeLa cells. Subsequently, confocal laser scanning microscopy was applied to investigate the ongoing interaction between the fluorescently labelled cell membrane and the green fluorescent S-liposomes. This study demonstrated that most of the S-liposomes were internalized within 2 hours of incubation and that the major part entered the HeLa cells by endocytosis [68]. To our knowledge, $rSbpA_{31\text{-}1068}$/EGFP is the first fusion protein that maintained the ability to fluorescence and to recrystallize into a monomolecular protein lattice. Due to the intrinsic fluorescence, liposomes coated with $rSbpA_{31\text{-}1068}$/EGFP represent a useful tool to visualize the uptake of S-liposomes into mammalian cells. The most interesting advantage can be seen in the recrystallization of fusion proteins incorporating EGFP in combination with HTs on the same liposome surface. In that case, it would be possible to simultaneously investigate the uptake of these specially coated S-liposomes by target cells and the functionality of transported drugs without the necessity of additional labelling procedures.

3.3. S-Layer Based Lipid Chips

Biological membranes have attracted lively interest, as the advances in genome mapping revealed that approximately one-third of all genes in an organism encode membrane proteins, such as ion channels, receptors, and membrane-bound enzymes [76]. In addition, more than 60 % of all consumed drugs act on membrane proteins [77]. Therefore, the generation of stabilized lipid membranes with functional membrane proteins represents a challenge to apply membrane proteins as key elements in drug discovery, protein-ligand screening and biosensors.

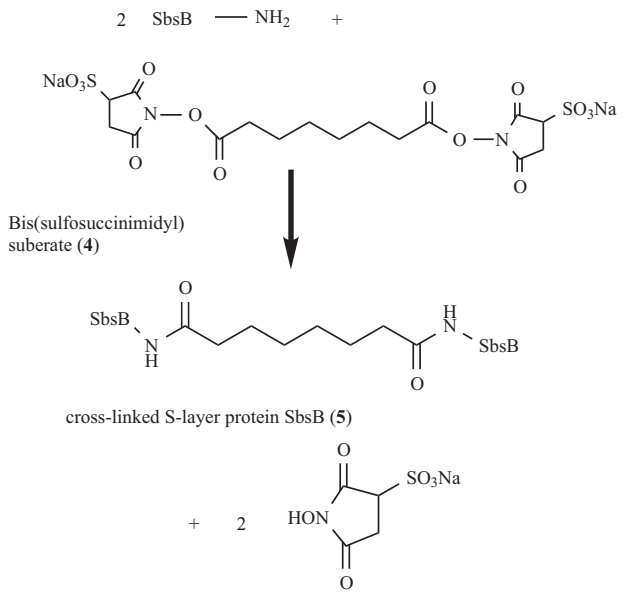

Fig. (6). Cross-linking of the S-layer protein SbsB with the water-soluble, homobifunctional N-hydroxysuccinimide-ester bis(sulfosuccinimidyl) suberate (BS_3; compound (**4**)). The spacer arm length of BS_3 is 1.14 nm.

S-layer-supported lipid membranes (SLM) mimic the supramolecular assembly of archaeal cell envelope structures, as they are composed of a cytoplasmic membrane and a closely associated S-layer [36]. In this biomimetic architecture, either a tetraetherlipid monolayer, or an artificial phospholipid bilayer replaces the cytoplasmic membrane and isolated bacterial S-layer proteins are attached either on one or both sides of the lipid membrane (Fig. **7**). The most commonly used lipids to generate planar SLMs are the phospholipid 1,2-diphytanoyl-*sn*-glycero-3-phosphatidylcholine (**6**), and the membrane-spanning tetraetherlipids Main Phospholipid (**7**) isolated from *Thermoplasma acidophilum* and glycerol dialkyl nonitol tetraetherlipid (**8**) extracted and purified from *Sulfolobus* and *Metallosphaera* archaea (Fig. **8**).

Electrostatic interactions between exposed carboxylic acid groups on the inner surface of the S-layer lattice and the zwitterionic lipid head groups were found to be primarily responsible for the defined binding of the S-layer subunits. As two to three contact points between the lipid film and the attached S-layer protein were determined, only few lipid molecules were anchored to protein domains on the S-layer lattice having a unit cell with a spacing of about 8 to 13 nm [78]. The remaining scores of lipid molecules diffused freely in the membrane between the pillars consisting of anchored lipid molecules. Because of its widely retained fluid characteristics, this nano-patterned lipid membrane was termed "semifluid membrane" [79]. But most important, although peptide side groups of the S-layer protein interpenetrated the phospholipid head group regions almost in its entire depth, no impact on the hydrophobic lipid alkyl chains was observed [80-83]. Thus, S-layer lattices constitute unique supporting scaffoldings for lipid membranes [36, 56, 84, 85].

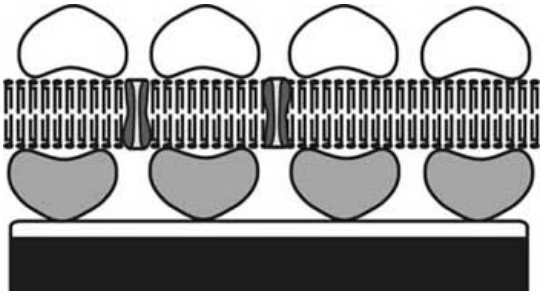

Fig. (7). Schematic drawing of an S-layer covered (modified) solid support (e.g. a gold electrode) carrying a lipid bilayer generated by vesicle fusion or by the Langmuir-Blodgett-technique. Integral membrane proteins can be reconstituted into this SLM. Furthermore, a second S-layer lattice can be recrystallized on the top of this biomimetic structure to provide an enhanced long-term stability and to act as a protective coat with pores in the nanometer range.

In reconstitution experiments, the self-assembly of the staphylococcal pore-forming protein α-hemolysin (αHL) [86] was examined at plain and SLMs [87]. αHL forms lytic pores when added to the lipid-exposed side of the S-layer-supported membrane. No assembly was detected upon adding αHL monomers to the S-layer-face of the composite membrane. Therefore, it was concluded that the intrinsic molecular sieving properties of the S-layer lattice did not allow the formation of αHL heptamers within the S-layer pores. Most interestingly, in SLMs the attached S-layer lattice caused a decreased tendency to rupture in the presence of αHL, indicating an enhanced stability [87]. Even single αHL pore recordings could be performed when reconstituted in S-layer supported lipid membranes [88].

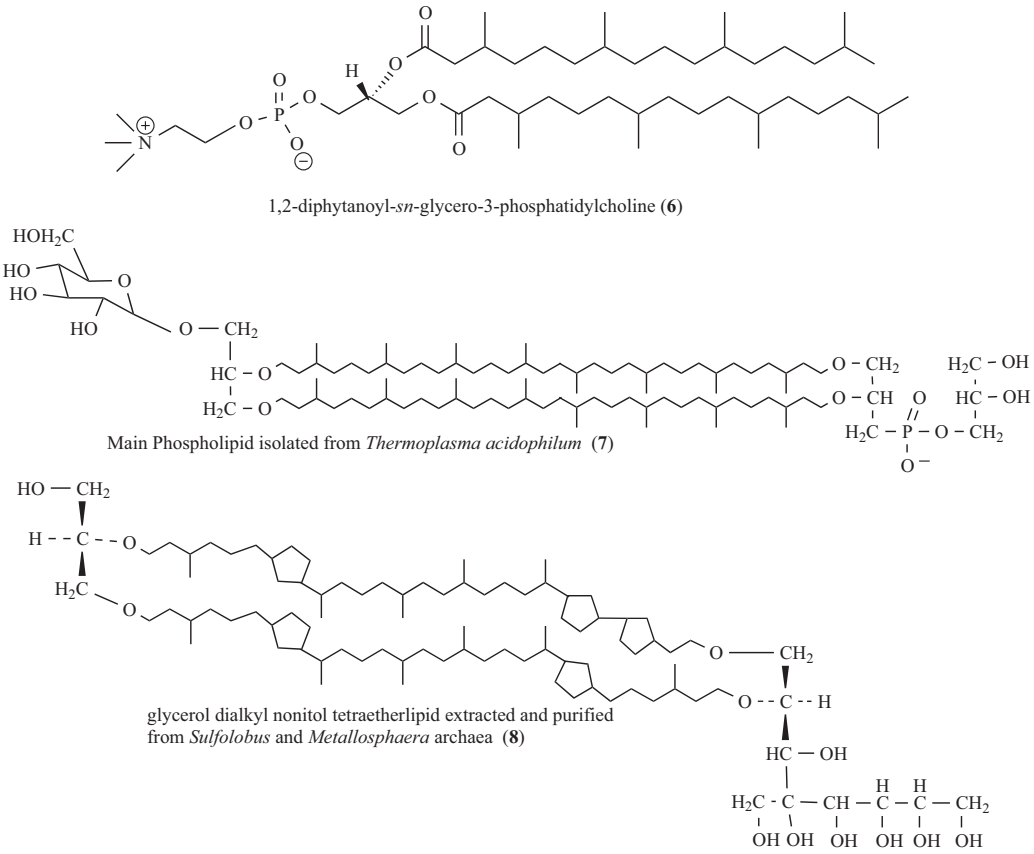

Fig. (8). Chemical structures of the phospholipid 1,2-diphytanoyl-*sn*-glycero-3-phosphatidylcholine (**6**), the membrane-spanning tetraetherlipids Main Phospholipid (**7**) isolated from *Thermoplasma acidophilum*, and glycerol dialkyl nonitol tetraetherlipid (**8**) extracted and purified from *Sulfolobus* and *Metallosphaera* archaea.

The functionality of lipid membranes resting on S-layer covered filters and gold electrodes was demonstrated by the reconstitution of αHL and membrane-active peptides [89, 90]. In a first study, gramicidin A was incorporated into tetraetherlipid monolayers, but also in phospholipid bilayers which were deposited on S-layer covered filters [89]. These membranes revealed not only a remarkable stability, particularly with an S-layer cover, but the most striking result was that high-resolution conductance measurements on single gramicidin pores were feasible. In addition, for the very first time, with filter supported lipid membranes, even single pore recordings were performed on reconstituted αHLs [91].

The functionality of lipid membranes resting on S-layer covered gold electrodes was demonstrated by the reconstitution of alamethicin, gramicidin and valinomycin [90]. Due to the formation of conductive alamethicin channels, the membrane resistance dropped two orders of magnitude whereas the capacitance was not altered. Partial inhibition of the alamethicin channels with amiloride and analogues was demonstrated, as increasing amounts of inhibitor gave rise to an increased membrane resistance [90]. In addition, an SLM surrounded by sodium buffer with incorporated valinomycin, a potassium-selective ion carrier, revealed a resistance in the GΩ-range. In contrast, for the same membrane bathed in potassium buffer the resistance dropped almost three orders of magnitude due to the valinomycin-mediated ion transport. These results demonstrated that the biomimetic approach of copying the supramolecular architecture of archaeal cell envelopes opened new possibilities for exploiting functional lipid membranes at meso- and macroscopic scale [92].

4. CONCLUSION AND FUTURE PERSPECTIVES

Basic and applied S-layer research has demonstrated that nature provides most elegant examples for nanometer sized, molecular self-assembly systems. There are only a few examples in nature where proteins reveal the intrinsic capability to self-assemble into crystalline arrays, in suspension and on a great variety of surfaces and interfaces. Since S-layer lattices are highly anisotropic structures with significant differences in the topography and physicochemical properties of the inner and outer surface, it was most important to copy nature's solution for assembling a secreted protein on the cell surface into lattices with defined

orientation. This biomimetic strategy is particularly essential to ensure that crystallization of genetically engineered S-layer proteins occurred in defined orientation on solid supports (metals, polymers, silicon wafers), lipid membranes, liposomes, and a great variety of nanoparticles [62-64].

Another line for exploiting the unique features of S-layers is directed to the use of lattices as support and stabilizing structures for functionalized lipid films and liposomes (Figs. **5** and **7**). Again, composite, semifluid SLMs are biomimetic structures copying the supramolecular principle of archaeal cell envelopes or human or animal virus envelopes optimized during biological evolution for a great variety of functions [5, 19, 36, 92].

The numerous benefits generated by the attachment of coherent S-layer lattices on lipid vesicles and mono- or bilayer membranes already triggered innovative approaches for membrane biosensors, high through-put screening, diagnostics, and different lab-on-a-chip designs. S-liposomes revealed high potentials for the development of new drug-targeting, drug-delivery and transfection systems [11, 20, 38, 40, 41, 43, 93].

Moreover, S-layer self-assembly products have been demonstrated to be particularly well-suited for a geometrically defined covalent attachment of haptens and immunogenic or immuno-stimulating substances [94]. Most recently, a remarkable immuno-modulating capacity of S-layers was demonstrated for a fusion protein comprising an S-layer protein from a Bacillaceae and the major birch pollen allergen Bet v 1 [67]. It is expected that innovative and highly specific immunogenic components with intrinsic targeting and delivery functionalities can be developed combining recombinant S-layer proteins with the supramolecular construction principle of virus envelopes (Fig. **6**).

Another attractiveness for S-layer self-assembly systems is seen for non-life science applications. Current state-of-the-art methods for self-assembly of nanoparticle arrays that generally involve bifunctional linkers, molecular recognition, or Langmuir-Blodgett techniques do not offer the control and flexibility of the S-layer system. The S-layer approach for the first time allows adjustable lattice constants and control over template surface properties by chemical or genetic modifications [5, 11, 15, 18] as required in molecular electronics, biocatalysis, and non-linear optics.

Currently, there is a strong need to improve and develop procedures for high resolution structural analysis of membrane proteins which can not be recrystallized to a quality suitable for X-ray analysis studies. By using S-layer fusion proteins, such target proteins could be forced into order arrays (Fig. **9**) [61] accessible for structural analysis involving established methods for image reconstruction such as high resolution (cryo) electron microscopy, X-ray and neutron reflectivity, and grazing incidence X-ray diffraction [81]. Intrinsic in plane distortions of lattices formed by S-layer fusion proteins can be corrected following standard procedures [23, 95].

It is now evident that S-layers represent unique patterning elements or base plates for a complex supramolecular construction kit (Fig. **9**). Although, a broad spectrum of applications for S-layers has been developed, it is expected that other areas will emerge particularly in areas where top-down and bottom-up strategies are commonly exploited.

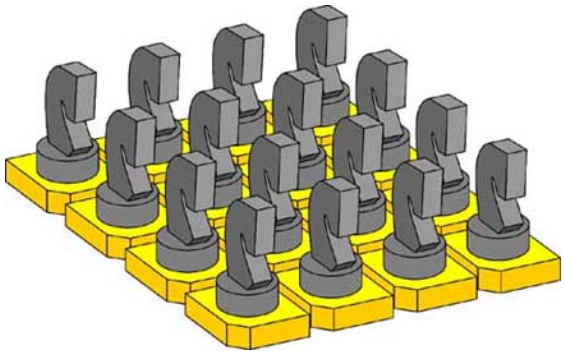

Fig. (9). Schematic drawing of an S-layer lattice (yellow chessboard) with regular and well orientated functional molecules (grey knights). The S-layer lattice of SbpA provides an area of up to 13 to 13 nm^2 for each functional molecule.

ACKNOWLEDGEMENTS

Financial support from the Austrian Science Fund (FWF, projects 16295-B10 and 17170-B10), the Erwin-Schrödinger Society for Nanosciences, the FP6 EC STREP NASSAP (project 13352), the Volkswagen Stiftung (project I/77710), and the Air Force Office of Scientific Research, USA (AFOSR, project F49620-03-1-0222) is gratefully acknowledged.

ABBREVIATIONS

Bet v 1	=	Major birch pollen allergen
BS_3	=	Bis(sulfosuccinimidyl) suberate
cAb	=	Variable domain of a heavy chain camel antibody
cAb-PSA-N7	=	cAb directed against the prostate-specific antigen
DMP	=	Dimethylpimelimidate
EGFP	=	Enhanced green fluorescent protein
GFP	=	Green fluorescent protein
HT	=	Heterotetramer
IgG	=	Immunoglobulin G
MDS	=	Microspheres-based detoxification system
PSA	=	Prostate-specific antigen
SbpA	=	S-layer protein of *Bacillus sphaericus* CCM2177
SbsB	=	S-layer protein of *Geobacillus stearothermophilus* PV72/p2
SbsC	=	S-layer protein of *Geobacillus stearothermophilus* ATCC 12980

SCWP	=	Secondary cell wall polymer
SFM	=	Scanning force microscopy
S-layer	=	Crystalline bacterial cell surface layer
SLH	=	S-layer-homology
S-liposome	=	S-layer coated liposome
SLM	=	S-layer supported lipid membrane
SPR	=	Surface plasmon resonance
TEM	=	Transmission electron microscopy
VHH	=	Variable domain of a heavy chain of a camel heavy chain antibody
Z-domain	=	Synthetic analogue of the (IgG)-binding B-domain of protein A of *Staphylococcus aureus*
ZZ	=	Two copies of the Z-domain

REFERENCES

[1] Sleytr, U.B. *Int. Rev. Cytol*., **1978**, *53*, 1.
[2] Sleytr, U.B.; Messner, P.; Minnikin, D.E.; Heckels, J.E.; Virji M.; Russell, R.B.B. In *Bacterial Cell Surface Techniques*, Hancock, I. C.; Poxton, I. Ed.; John Wileys & Son, Chichester, **1988**; pp. 1-31.
[3] Sleytr, U.B. *FEMS Microbiol. Reviews* **1997**, *20*, 5.
[4] Sleytr, U.B.; Beveridge, T.J. *Trends Microbiol.*, **1999**, *7*, 253.
[5] Sleytr, U.B.; Messner, P.; Pum, D.; Sára, M. *Angew. Chem. Int. Ed*., **1999**, *38*, 1034.
[6] König, H. *Can. J. Microbiol*., **1988**, *34*, 395.
[7] Beveridge, T.J. *Int Rev Cytol*., **1981**, *72*, 229.
[8] Baumeister, W.; Lembecke, G. *J. Bioenerg. Biomembr*., 1992, *24*, 567.
[9] Sára, M.; Sleytr, UB. *J. Bacteriol*., **2000**, *182,* 859.
[10] Messner, P.; Sleytr, U.B. *Adv. Microb. Physiol*., **1992**, *33*, 213.
[11] Sleytr, U.B.; Sára, M.; Pum, D.; Schuster, B. In *Supramolecular Polymers 2*, Ciferri, A. Ed.; Marcel Dekker: New York, Basel, **2005**; pp. 583.
[12] Sára, M.; Egenseer, E.-M. In *Crystalline Bacterial Cell Surface Proteins*, Sleytr, U.B.; Messner, P.; Pum, D.; Sára, M. Eds.; Academic Press: Austin, **1996**; pp. 103.
[13] Sára, M. *Trends Microbiol*., **2001**, *9*, 47.
[14] Sára, M.; Sleytr, U.B. *J. Bacteriol*., **1987**, *169*, 4092.
[15] Sleytr, U.B.; Sára, M.; Pum, D.; Schuster, B.; Messner, P.; Schäffer, C. In *Biopolymers,* Steinbüchel, A.; Fahnestock, S. Eds.; Wiley-VCH: Weinheim, **2002**; Vol. *7*, pp. 285.
[16] Messner, P.; Pum, D.; Sára, M.; Stetter, K.O.; Sleytr, U.B. *J. Bacteriol*., **1986**, *166*, 1046.
[17] Pum, D.; Messner P.; Sleytr, U.B. *J. Bacteriol*., **1991**, *173*, 6865.
[18] Sleytr, U.B.; Pum, D.; Sára, M.; Schuster, B. In *Encyclopedia of Nanoscience and Nanotechnology,* Nalwa, H.S. Ed.; Academic Press, San Diego, **2004**; pp 693.
[19] Sleytr, U.B.; Egelseer, E.-M.; Pum, D.; Schuster, B. In: *NanoBiotechnologie: Concepts, Methods and Perspectives,* Niemeyer, C. M.; Mirkin, C. A. Eds.; Wiley-VCH: Weinheim, Germany, **2004**, pp. 77.
[20] Sleytr, U.B.; Sára, M.; Pum, D.; Schuster, B. In *Nano-surface chemistry*, Rosoff, M. Ed.; Marcel Dekker, Inc.: New York, **2001**, pp. 333.
[21] Sleytr, U.B.; Sára, M.; Pum, D.; Schuster, B. *Prog. Surf. Sci.*, **2001**, *68*, 231.
[22] Robards, A.W.; Sleytr, U.B. In *Practical Methods in Electron Microscopy*; Glauert, A.M. Ed.; Elsevier Sciences B. V: Amsterdam, **1985**; Vol. *10*.
[23] Baumeister, W.; Engelhardt, H. In *Electron Microscopy of Proteins*; Harris J.R.; Horne, R.W. Eds.; Academic Press: London, **1987**; Vol. *6*, pp. 109.
[24] Hovmöller, S.; Sjögren, A.; Wang, D.N. *Prog. Biophys. Mol. Biol*., **1988**, *51*, 131.
[25] Amos, L.A.; Henderson, R.; Unwin, P.N.T. *Progr. Biophys. Mol. Biol*., **1982**, *39*, 183.
[26] Györvary, E.S.; Stein, O.; Pum, D.; Sleytr, U.B. *J. Microsc*., **2003**, *212*, 300.
[27] Karrasch, S.; Hegerl, R.; Hoh, J.;, Baumeister, W.; Engel, A. *Proc. Natl. Acad. Sci. USA*, **1994**, *91*, 836.
[28] Pum, D.; Sleytr, U.B. *Supramol. Sci*., **1995**, *2*, 193.
[29] Müller, D.J.; Baumeister, W.; Engel, A. *J. Bacteriol*., **1996**, *178*, 3025.
[30] Scheuring, S.; Stahlberg, H.; Chami, M.; Houssin, C.; Rigaud, J.L.; Engel, A. *Mol. Microbiol*., **2002**, *44*, 675.
[31] Stroh, C.M.; Ebner, A.; Geretschläger, M.; Freudenthaler, G.; Kienberger, F.; Kamruzzahan, A.S.M.; Smith-Gill, S.J.; Gruber, H.J.; Hinterdorfer, P. *Biophys. J*., **2004**, *87*, 1981.
[32] Sleytr, U.B.; Messner, P. In *Electron Microscopy of Subcellular Dynamics*; Plattner, H. Ed.; CRC Press: Boca Raton, FL, **1989**; pp 13.
[33] Ilk, N.; Kosma, P.; Puchberger, M.; Egelseer, E.M.; Mayer, H.F.; Sleytr, U.B.; Sára, M. *J. Bacteriol*., **1999**, *181*, 7643.
[34] Howorka, S.; Sára, M.; Wang, Y.; Kuen, B.; Sleytr, U.B.; Lubitz, W.; Bayley, H. *J. Biol. Chem*., **2000**, *275*, 37876.
[35] Sára, M.; Dekitsch, C.; Mayer, H.F.; Egelseer, E.M.; Sleytr, U.B. *J. Bacteriol*., **1998**, *180*, 4146.
[36] Schuster, B.; Sleytr, U.B. *Rev. Molec. Biotechnol*., **2000**, *74*, 233.
[37] Pum, D.; Weinhandl, M.; Hödl, C.; Sleytr, U.B. *J. Bacteriol*., **1993**, *175*, 2762.
[38] Küpcü, S.; Sára, M.; Sleytr, U.B. *Biochim. Biophys. Acta*, **1995**, *1235*, 263.
[39] Mader, C.; Küpcü, S.; Sára, M.; Sleytr, U.B. *Biochim. Biophys. Acta*, **1999**, *1418*, 106.
[40] Mader, C.; Küpcü, S.; Sleytr, U.B.; Sára, M. *Biochim. Biophys. Acta*, **2000**, *1463*, 142.
[41] Toca-Herrera, J. L.; Krastev, R.; Bosio, V.; Küpcü, S.; Pum, D.; Fery, A.; Sára, M.; Sleytr, U. B. *Small*, **2005**, *1*, 339.
[42] Toca-Herrera, J. L.; Moreno-Flores, S.; Friedmann, J.; Pum, D.; Sleytr, U. B. *Microsc. Res. Tech.*, **2004**, *66*, 163.
[43] Sára, M.; Pum, D.; Schuster, B.; Sleytr, U.B. *J. Nanosci. Nanotechnol*., **2005**, *5*, 1936.
[44] Huber, C.; Ilk, N.; Rünzler, D.; Egelseer, E.-M.; Weigert, S.; Sleytr, U.B.; Sára, M. *Mol. Microbiol*., **2005**, *55*, 197.
[45] Ilk, N.; Völlenkle, C.; Egelseer, E.-M.; Breitwieser, A.; Sleytr, U.B.; Sára, M. *Appl. Environ. Microbiol*., **2002**, *68*, 3251.
[46] Jarosch, M.; Egelseer, E.-M.; Huber, C.; Moll, D.; Mattanovich, D.; Sleytr, U.B.; Sára, M. *Microbiology*, **2001**, *147*, 1353.
[47] Pavkov, T.; Oberer, M.; Egelseer, E.-M.; Sára, M.; Sleytr, U.B.; Keller, W. *Acta Crystallogr. D Biol. Crystallogr.*, **2003**, *59*, 1466.
[48] Steindl, C.; Schäffer, C.; Wugeditsch, T.; Graninger, M.; Matecko, I.; Müller, N.; Messner, P. *Biochem. J*., **2002**, *368*, 483.
[49] Schäffer, C.; Messner, P. *Microbioogy,* **2005**, *151*, 643.
[50] Cava, F.; de Pedro. M.A.; Schwarz, H.; Henne, A.; Berenguer, *J. Mol. Microbiol*., **2004**, *52*, 677.
[51] Mesnage, S.; Fontaine, S.; Mignot, T.; Delepierre, M.; Mock, M.; Fouet, A. *EMBO J*., **2000**, *19*, 4473.
[52] Egelseer, E.-M.; Leitner, K.; Jarosch, M.; Hotzy, C.; Zayni, S.; Sleytr, U.B.; Sára, M. *J. Bacteriol*. **1998**, *180*, 1488.
[53] Jarosch, M.; Egelseer, E.-M.; Mattanovich, D.; Sleytr, U.B.; Sára, M. *Microbiology,* **2000**, *146*, 273.
[54] Egelseer, E.-M.; Danhorn, T.; Pleschberger, M.; Hotzy, C.; Sleytr, U.B.; Sára, M. *Arch. Microbiol*., **2001**, *177*, 70.
[55] Messner, P.; Sleytr, U.B.; Christian, R.; Schulz, G.; Unger, F.M. *Carbohydr. Res*., **1987**, *168*, 211.
[56] Schäffer, C.; Kählig, H.; Christian, R.; Schulz, G.; Zayni, S.; Messner, P. *Microbiology*, **1999**, *145*, 1575.
[57] Pum, D.; Schuster, B.; Sára, M.; Sleytr, U.B. *IEE Proc. Nanobiotech*., **2004**, *151*, 83.
[58] Schuster, B.; Gufler, P.C.; Pum, D.; Sleytr, U.B. *IEEE Trans. Nanobiosci*., **2004**, *3*, 16.
[59] Bayley, H.; Braha, O.; Cheley, S.; Gu, L.-Q. In *NanoBiotechnology: Concepts, Methods and Perspectives*, Niemeyer, C.M.; Mirkin C.A. Eds.; Wiley-VCH Verlag: Weinheim; **2004**; pp. 93-112.
[60] Huber, C.; Liu, L.; Egelseer, E.-M.; Moll, D.; Knoll, W.; Sleytr, U.B.; Sára, M. *Small*, **2006**, *2*, 142.
[61] Moll, D.; Huber, C.; Schlegel, B.; Pum, D.; Sleytr, U.B.; Sára, M. *Proc. Natl. Acad. Sci. USA*, **2002**, *99*, 14646.

[62] Pleschberger, M.; Neubauer, A.; Egelseer, E.-M.; Weigert, S.; Lindner, B.; Sleytr, U.B.; Muyldermans, S.; Sára, M. *Bioconj. Chem*., **2003**, *14*, 440.
[63] Pleschberger, M.; Saerens, D.; Weigert, S.; Sleytr, U.B.; Muyldermans, S.; Sára, M.; Egelseer, E.-M. *Bioconj. Chem*., **2004**, *15*, 664.
[64] Völlenkle, C.; Weigert, S.; Ilk, N.; Egelseer, E.-M.; Weber, V.; Loth, F.; Falkenhagen, D.; Sleytr, U.B.; Sára, M. *Appl. Environ. Microbiol*., **2004**, *70*, 1514. Highlighted in *Nat. Rev. Microbiol*., **2004**, *2*, 353.
[65] Weber, V.; Weigert, S.; Sára, M.; Sleytr, U.B.; Falkenhagen, D. *Ther. Apher.*, **2001**, *5*, 433.
[66] Breitwieser, A.; Egelseer, E.-M.; Ilk, N.; Moll, D.; Hotzy, C.; Bohle, B.; Ebner, C.; Sleytr, U.B.; Sára, M. *Protein Eng*., **2002**; *15*, 243.
[67] Bohle, B.; Breitwieser, A.; Zwölfer, B.; Jahn-Schmid, B.; Sára, M.; Sleytr, U.B.; Ebner, C. *J. Immunol*., **2004**, *172*, 6642.
[68] Ilk, N.; Küpcü, S.; Moncayo, G.; Klimt, S.; Ecker, R.; Hofer-Warbinek, R.; Egelseer, E.-M.; Sleytr, U.B.; Sára, M. *Biochem. J*., **2004**, *370*, 441.
[69] Crommelin, D.; Storm, G. *J. Liposome Res*., **2003**, *13*, 33.
[70] Lasic, D.D.; Papahadjopoulos, D. *Science*, **1995**, *267*, 1275.
[71] Torchilin, V.P. *Nat. Rev. Drug Discov*., **2005**, *4*, 145.
[72] Lasic, D.D. *Trends Biotechnol*., **1998**, *16*, 307.
[73] Templeton, N.S.; Lasic, D.D. *Mol. Biotechnol*., **1999**, *11*, 175.
[74] Ostro, M.J.; Cullis, P.R. *Am. J. Hosp. Pharm*., **1989**, *46*, 1576.
[75] Küpcü, S.; Lohner, K.; Mader, C.; Sleytr, U.B. *Mol. Membr. Biol*., **1998**, *15*, 69.
[76] Gerstein, M.; Hegyi, H. *FEMS Microbiol. Rev.,* **1998**, *22*, 277.
[77] Ellis, C.; Smith, A. *Nature Rev. Drug Disc.,* **2004**, *3*, 237.
[78] Wetzer, B.; Pfandler, A.; Györvary, E.; Pum, D.; Lösche, M.; Sleytr, U.B. *Langmuir,* **1998**, *14*, 6899.
[79] Pum, D.; Sleytr, U.B. *Thin Solid Films*, **1994**, *244*, 882.
[80] Schuster, B.; Pum, D.; Sleytr, U.B. *Biochim. Biophys. Acta*, **1998**, *1369,* 51.
[81] Weygand, M.; Wetzer, B.; Pum, D.; Sleytr, U.B.; Cuvillier, N.; Kjaer, K.; Howes, P.B.; Lösche, M. *Biophys. J*., **1999**, *76*, 458.
[82] Weygand, M.; Schalke, M.; Howes, P.B.; Kjaer, K.; Friedmann, J.; Wetzer, B.; Pum, D.; Sleytr, U.B.; Lösche, M. *J. Mater. Chem*., **2000**, *10*, 141.
[83] Weygand, M.; Kjaer, K.; Howes, P.B.; Wetzer, B.; Pum, D.; Sleytr, U.B.; Lösche, M. *J. Phys. Chem. B.,* **2002**, *106*, 5793
[84] Schuster, B.; Gufler, P.C.; Pum, D.; Sleytr, U.B. *Langmuir*, **2003**, *19*, 3393.
[85] Schuster, B.; Sleytr, U.B. *Biochim. Biophys. Acta,* **2002**, *1563*, 29.
[86] Bhakdi, S.; Tranum-Jensen, J. *Microbiol. Rev.*, **1991**, *55*, 733.
[87] Schuster, B.; Pum, D.; Braha, O.; Bayley, H.; Sleytr, U.B. *Biochim. Biophys. Acta,* **1998**, *1370*, 280.
[88] Schuster, B.; Sleytr, U.B. *Bioelectrochemistry*, **2002**, *55*, 5.
[89] Schuster, B.; Weigert, S.; Pum, D.; Sára, M.; Sleytr, U.B. *Langmuir*, **2003**, *19*, 2392.
[90] Gufler, P.C.; Pum, D.; Sleytr, U.B.; Schuster, B. *Biochim. Biophys. Acta*, **2004**, *1661*, 154.
[91] Schuster, B.; Pum, D.; Sára, M.; Braha, O.; Bayley, H.; Sleytr, U. B. *Langmuir*, **2001**, *17*, 499.
[92] Schuster, B. *NanoBiotechnology*, **2005**, *1*, 153.
[93] Schuster, B.; Sleytr, U.B. In *Advanves in Planar Lipid Bilayers and Liposomes*, Tien, T.H.; Ottova, A. Eds.; Elsevier Science: Amsterdam, **2005**; Vol. *1*, pp. 247-293.
[94] Jahn-Schmid, B.; Graninger, M.; Glozik, M.; Küpcü, S.; Ebner, C.; Unger, F.M.; Sleytr, U.B.; Messner, P. *Immunotechnology*, **1996**, *2*, 103.
[95] Crowther, R.A.; Sleytr, U.B. *J. Ultrastruct. Res*., **1977**, *58*, 41.

Received: November 10, 2005 Revised: January 17, 2006 Accepted: January 18, 2006